Writing and applications fibre Bragg grating arrays

S. La Rochelle, P.-Y. Cortès, H. Fathallah, L.A. Rusch, and H. Ben Jaafar

Centre d'optique, photonique et laser (COPL)
Département de génie éléctrique et de génie informatique
Université Laval, Québec, Canada G1K 7P4
larochel@gel.ulaval.ca

Abstract

Multiple Bragg gratings are written in a single fibre strand with accurate positioning to achieve predetermined time delays between optical channels. Applications of fibre Bragg grating arrays include encoders/decoders with series of identical gratings for optical code-division multiple access.

Keywords: Optical fibre component, Bragg grating, grating array, multi-frequency grating, multi-wavelength grating, code-division multiple access, CDMA, OCDMA

1. Introduction

Over the last decade, fibre Bragg gratings have found increasing applications in wavelength division multiplexed (WDM) optical communication systems[1]. Diode laser stabilisation and channel filtering for add/drop modules are some of the most common functions performed by fibre gratings[2]. In these situations, Bragg gratings are designed as independent narrowband filters and multiple channel filters can be realised by concatenation of the gratings. Fibre gratings are also widely used for gain equalisation, while chirped fibre Bragg gratings are extensively studied for chromatic dispersion compensation. In the latter case, particular attention is paid to the time delay between the reflected frequencies of the wideband grating. It was recently demonstrated that the control of the reflection time delays introduced by separate narrowband fibre Bragg gratings is also beneficial to the performance of optical communication systems. Inducing time delays between adjacent channels, by adequate positioning of Bragg gratings along an optical fibre, was shown to lower the penalties resulting from cross-phase modulation (XPM) in 10 Gb/s WDM systems[3]. Furthermore, writing series of fibre Bragg gratings along a fibre allows a new implementation of optical code-division multiple access (OCDMA) using a two-dimension, frequency and time, coding space[4-5].

In this paper, we discuss the writing and application of Bragg grating arrays (BGA) written in the same optical fibre. The BGA, with reflection peaks spaced by 100 GHz and 50 GHz, are designed to introduce specific time delays between the reflected frequency bands. The writing of BGA with a Sagnac type interferometer is described in section 2. This method combines the wavelength flexibility of interferometric techniques with the ability to write longer gratings of standard phase-mask scanning setups. The characteristics of the BGA series, realised to suppress cross-phase modulation, are presented in the following section. Applications of BGA are discussed in section 4 with emphasis on OCDMA. In this experiment, four decoders made from BGA, consisting of series of eight gratings, were stretched-tuned to isolate the desired signal from sixteen simultaneously transmitted users. The signal from each user was encoded using the same type of BGA with eight gratings.

2. Writing Bragg gratings with a Sagnac-type interferometer

Several methods have been proposed to tune the Bragg wavelength of fibre gratings during UV exposure. Interferometric techniques[6-8], such as the two-mirror interferometer originally proposed by Meltz et al.[6] or the classical Lloyd configuration[7], are often used to write short gratings with lengths usually less than 1 cm[6-8]. Longer gratings can be obtained by concatenation of these small gratings. Controlled motion of the optical fibre, usually obtained by interferometric sensing, is then required to achieve precise positioning of the grating elements[9]. When using phase mask scanning techniques[10-11], tuning of the Bragg wavelength can be achieved over a limited range[12-16], typically less than 10 nm. Methods that have been proposed to control

Applications of Photonic Technology 4, Roger A. Lessard, George A. Lampropoulos, Editors, Proceedings of SPIE Vol. 4087 © 2000 SPIE · 0277-786X/00/$15.00

the Bragg wavelength include tilting the fibre[12], rotating the scanning mirror[13], stretching the fibre[14], varying the curvature of the writing wavefront[15] or moving the fibre relative to the phasemask[16]. The Sagnac-type interferometer, originally proposed by Ouellette and Krug[17], combines the flexibility of interferometric technique, by allowing tuning of the Bragg wavelength over a wide range, and the advantage of phase mask scanning techniques in producing good quality longer gratings. It has some similarities to a folded version of the Talbot interferometer proposed by Kahsyap[18].

The Sagnac interferometer used to write BGA is presented in Fig.1. In this method, the phase mask diffracts the light in the ±1 orders thereby producing two counter-propagating beams in the interferometer. The optical fibre is placed slightly above the phase-mask and a small out-of-plane tilt is introduced to the two mirrors to recombine the UV beams at the optical fibre position. Since both diffracted beams interact with the two mirrors, this interferometer is immune to some vibration modes of the mirrors and a stable interferometer can easily be realised. Any UV light diffracted to higher orders or remaining in the zero order is eliminated by this configuration. A cylindrical lens is introduced between the mirrors to focus the light along the optical fibre axis. When scanning of the phase mask is performed, the exposed region of the fibre moves in opposite direction to the translation of the UV beam. As in other interferometric methods, variation of the angle between the two interfering beams results in a modification of the photo-induced grating period. In this case, the Bragg wavelength, λ_B, changes according to

$$\lambda_B = \frac{n_{eff}\lambda_{UV}}{\sin(\pi - 2\varphi_1 - 2\varphi_2 - \theta)},$$

where n_{eff} is the effective index of the guided mode, λ_{UV} is the writing wavelength, φ_1 and φ_2 the mirror angles. When simultaneously moving both mirrors ($\varphi_1=\varphi_2=\varphi$), the Bragg wavelength tuning is

$$\frac{\Delta\lambda_B}{\lambda_B} = 4\cot(\pi - 4\varphi - \theta)\,\Delta\varphi \quad .$$

When $\varphi_1=\varphi_2=(\pi/4)-(\theta/2)$ the interference occurs directly above the phase-mask and the Bragg wavelength is given by the usual expression $\lambda_B = n_{eff}\Lambda_{PM}$, where Λ_{PM} is the phase-mask period. With a typical phase mask period of $\Lambda_{PM}\approx1070$ nm, the angular sensitivity of λ_B is typically $\delta\lambda_B/\delta\phi\approx460$ nm/deg. The Bragg wavelength is presented in Fig. 2 as a function of the angle of the mirrors. Theoretically, Bragg wavelengths from 800 nm to more than 2 μm could be obtained using this interferometric setup. In practice, in the telecommunication window, wavelength tuning can be performed by rotating only one of the mirror, leading to $\delta\lambda_B/\delta\phi\approx230$ nm/deg as shown in the inset of Fig. 2. Introducing a 42 cm lever beam, controlled by a nanomover with a 50-nm resolution, angular steps of $\Delta\phi_1=7.10^{-6}$ deg can be achieved and a chirped Bragg grating can be written by rotating the mirror as the fibre is scanned. The amplitude and delay of such a chirped Bragg grating is shown in Fig. 3. It should be noted that the fibre grating length, L_g, is limited by the aperture of the interferometer mirrors and typically $L_g \approx \Phi_M \sin(\pi/4 + \theta)/\sin(\pi/2 - \theta) \approx 0.8\,\Phi_M$, where Φ_M is the mirror diameter.

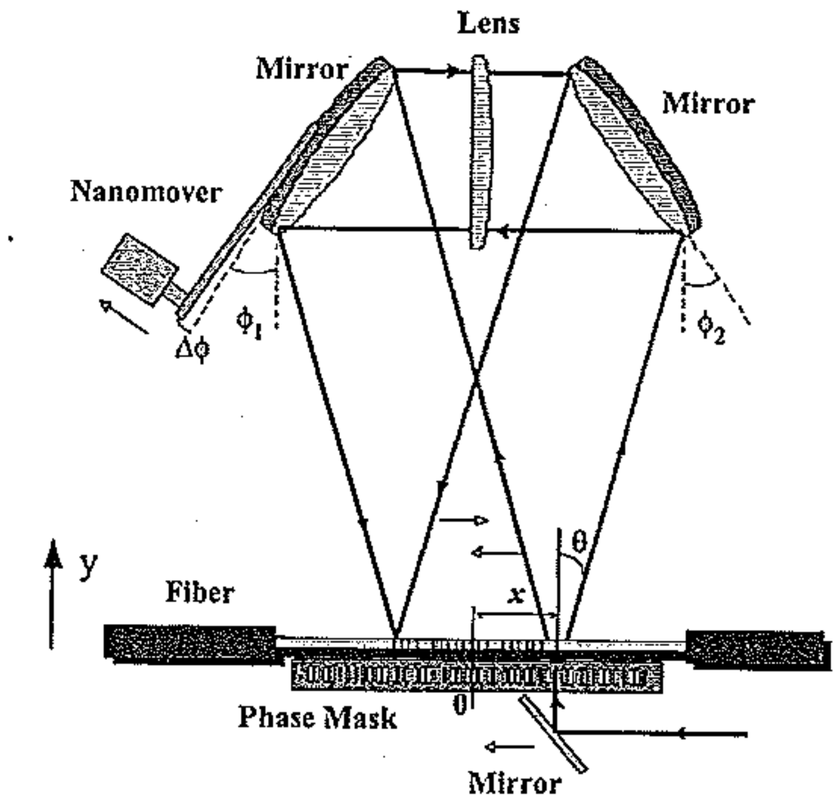

Fig. 1 Sagnac-type interferometric setup.

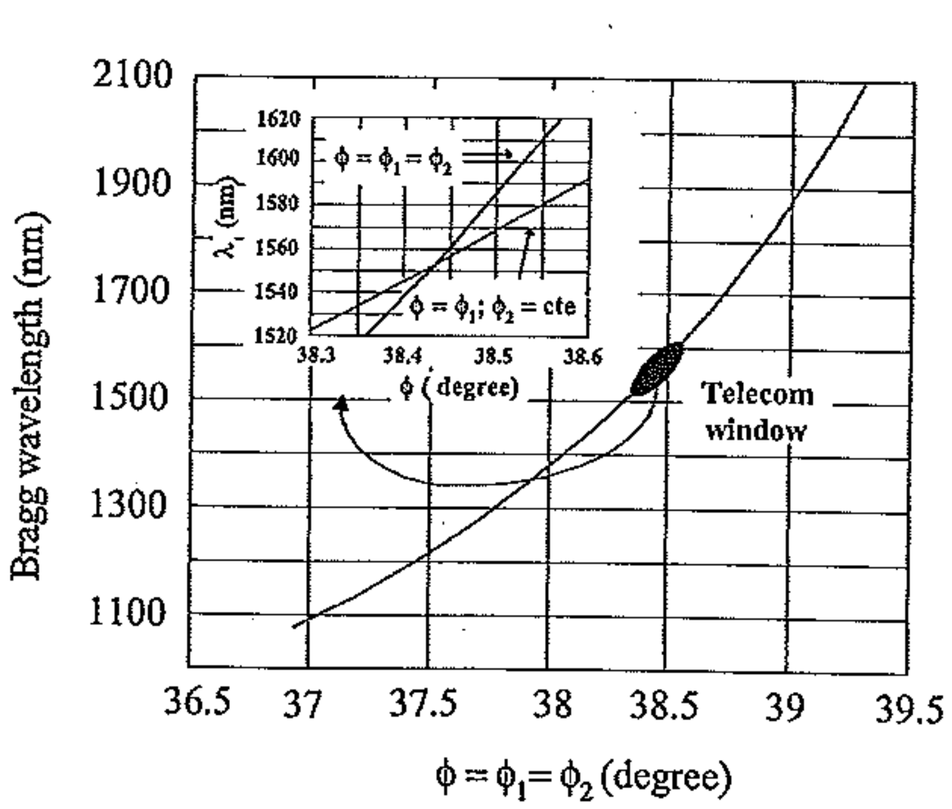

Fig. 2 Tuning of the Bragg wavelength as a function of the mirror angles.

The grating length is also reduced as the mirror angle is changed. As displayed in Fig. 4 , the grating length is 4 cm around 1.55 μm and 3.7 cm around 1.3 μm for 5 cm diameter mirrors using a phase mask designed for a 1.55 μm Bragg wavelength. On Fig. 4, it can also be observed that the interference pattern position moves forward or backward with respect to the phase mask, along the y-axis, as the mirror angle varies.

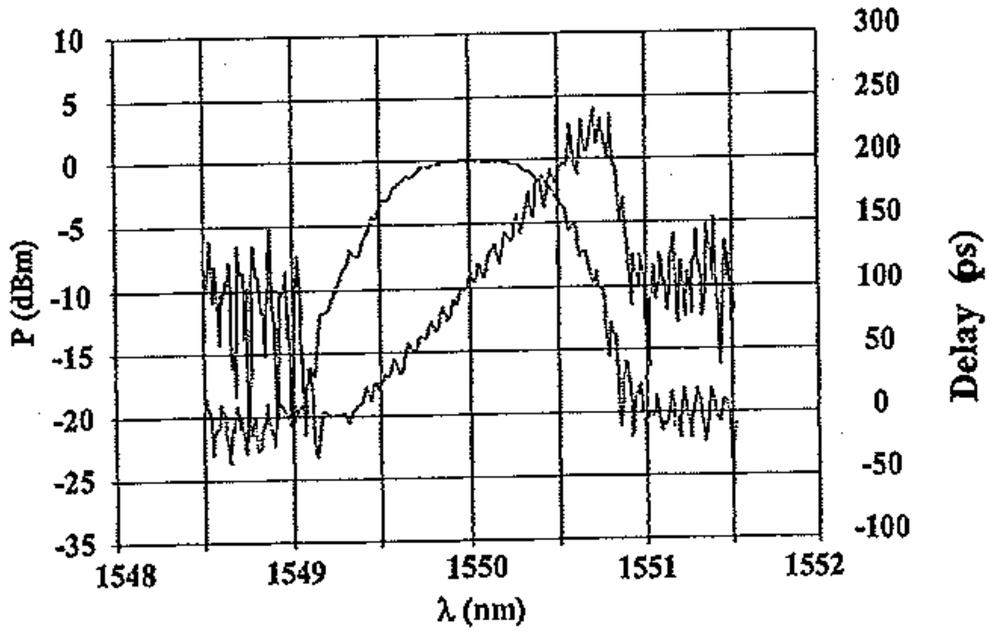

Fig. 3 Reflected power and delay of a chirped Bragg grating.

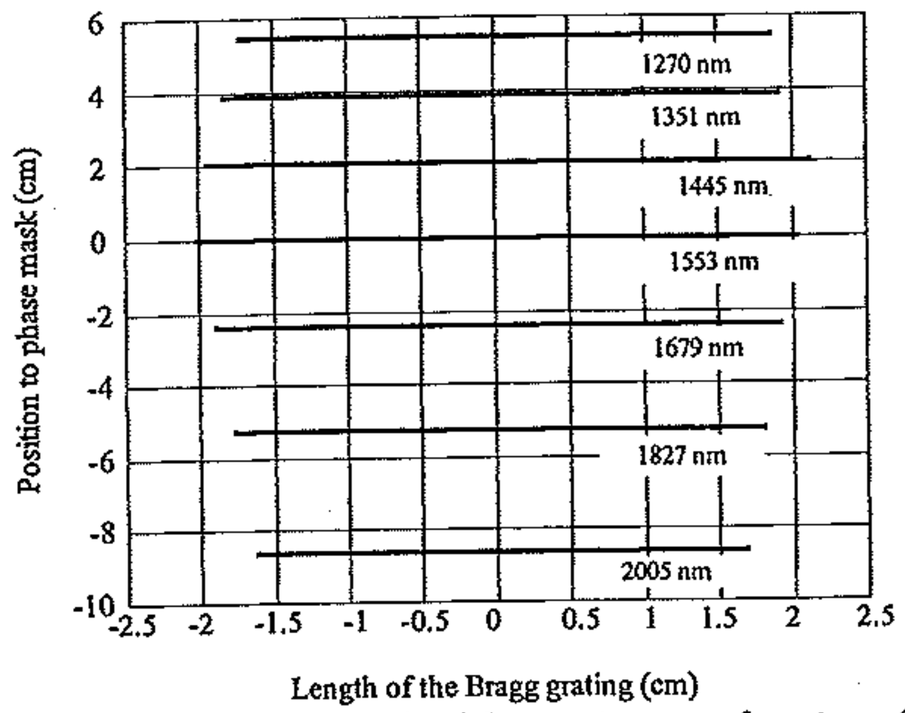

Fig. 4 Position and length of the grating as a function of the chosen Bragg wavelength.

Two types of lasers were used to write fibre gratings using this setup: a pulsed frequency-quadrupled CW-mode locked Nd:Yag laser and a CW frequency doubled Argon-ion laser. The mode-locked laser produced 266 nm pulses of 60 ps FWHM at a repetition rate of 80 MHz with an average UV power of 70 mW. The frequency-doubled argon-ion laser delivered up to 150 mW of average power. The temporal characteristic of the writing beam has an important impact on the profile of the resulting grating. From Fig.1, it can be observed that there is an optical path length difference (OPD) between the co-propagating and the counter-propagating beams when the UV beam is moved away from the centre of the phase-mask. Noting the position of the scanning beam from the central plane of the interferometer by x, the optical path length difference is given by $\Delta\delta(x) = 2x(1-2\sin\theta)$. As the pulsed UV source is scanned across the phase-mask, a temporal walk-off is introduced at the interference plane between the pulses propagating in the clockwise and the counter-clockwise direction. Therefore, although the same amount of energy is delivered to the optical fibre, the visibility of the fringes will vary. Hence, automatic apodisation of the Bragg gratings occur with a function corresponding to the auto-correlation of the writing pulses as the OPD increases[19]. With 60 ps pulses, the OPD at the mirror edges was not sufficient to totally separate the optical pulses and a truncated gaussian apodisation function, displayed in Fig.5a, was obtained. The reflection amplitude of the apodised grating is show in Fig.5b along with the calculated reflectivity profile and the calculated spectra of an unapodised grating. The grating was written in an hydrogen-loaded fibre. The reflectivity spectrum and the 3 dB bandwidth of 0.26 nm indicate an index change of the order of 3.4×10^{-4}. To obtain arbitrary apodisation functions or to write short apodised Bragg gratings, the interferometric writing technique can be combined to the double exposure methods to obtained the desired apodisation profile. Typically, when using the CW laser, a first exposure with a varying scanning speed function is done to write the grating an a second exposure with the inverse velocity profile is performed, while vibrating the phase-mask, to raise the average refractive index.

Series of BGA are written in optical fibres in a sequential fashion. After the writing of the first grating, the optical fibre is moved to a new location, the angle of the mirror is modified to choose the new wavelength and the new grating is written at the centre of the interferometer. The precision on the optical fibre translation is better than 25 μm. Because of the necessary adjustments and alignments of the interferometer, the Bragg wavelength accuracy for the first grating is ±0.25 nm while the precision on the Bragg wavelength steps for the following gratings is ±0.04 nm. The long focal length of the cylindrical lens, here 28 cm, results in a low power density at the optical fibre location. Therefore, hydrogen-loaded fibres must be used to obtain sufficient index change at reasonable scanning speed with a single exposure.

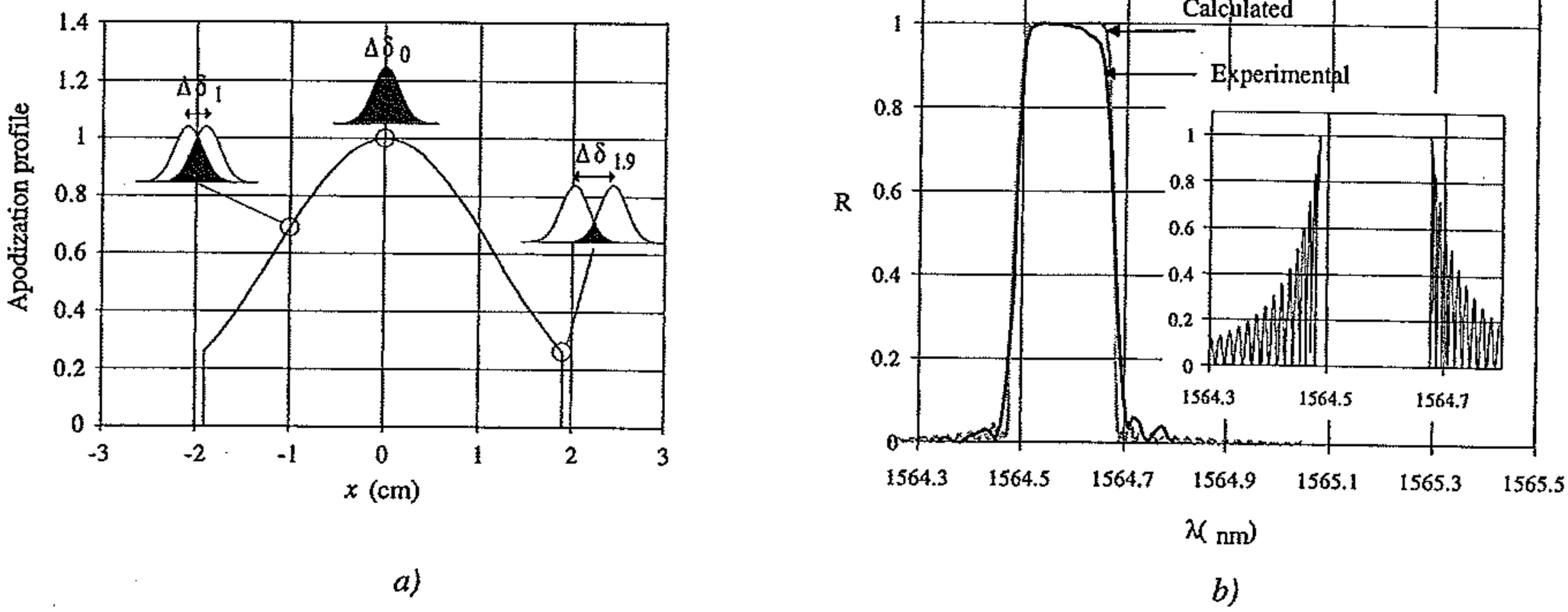

a) *b)*

Fig. 5: Gaussian apodisation of fibre Bragg gratings resulting from pulse walk-off along the fibre length a) apodisation profile and b) experimental and calculated reflectivity. The inset show the calculated reflectivity for a uniform grating calculated with the same index change of 3.4×10^{-4}.

3.Characteristics of Bragg gratings arrays (BGA)

Four identical series of Bragg gratings arrays with ten reflection peaks spaced by 100 GHz were written using the described interferometric setup with the CW frequency-doubled Argon-ion laser. The lengths of the gratings were 5 mm with a sinc main lobe apodisation function. The spacing between the gratings varied between 10 mm and 6.6 mm to optimise the suppression of the XPM effects on the transmission of ten channels at 10 Gb/s [3]. Fig.6a shows the spectral characteristics, reflected power and delay, of one of these series. The measured wavelength separation was 0.80 nm ± 0.04 nm and the 3 dB FWHM was 0.42 nm ± 0.01 nm. The reflectivity of the first grating was near 14 dB and photo-induced loss of 0.3 dB/ grating was observed. The calculated amplitude of the refractive index change is 6.4×10^{-4}.

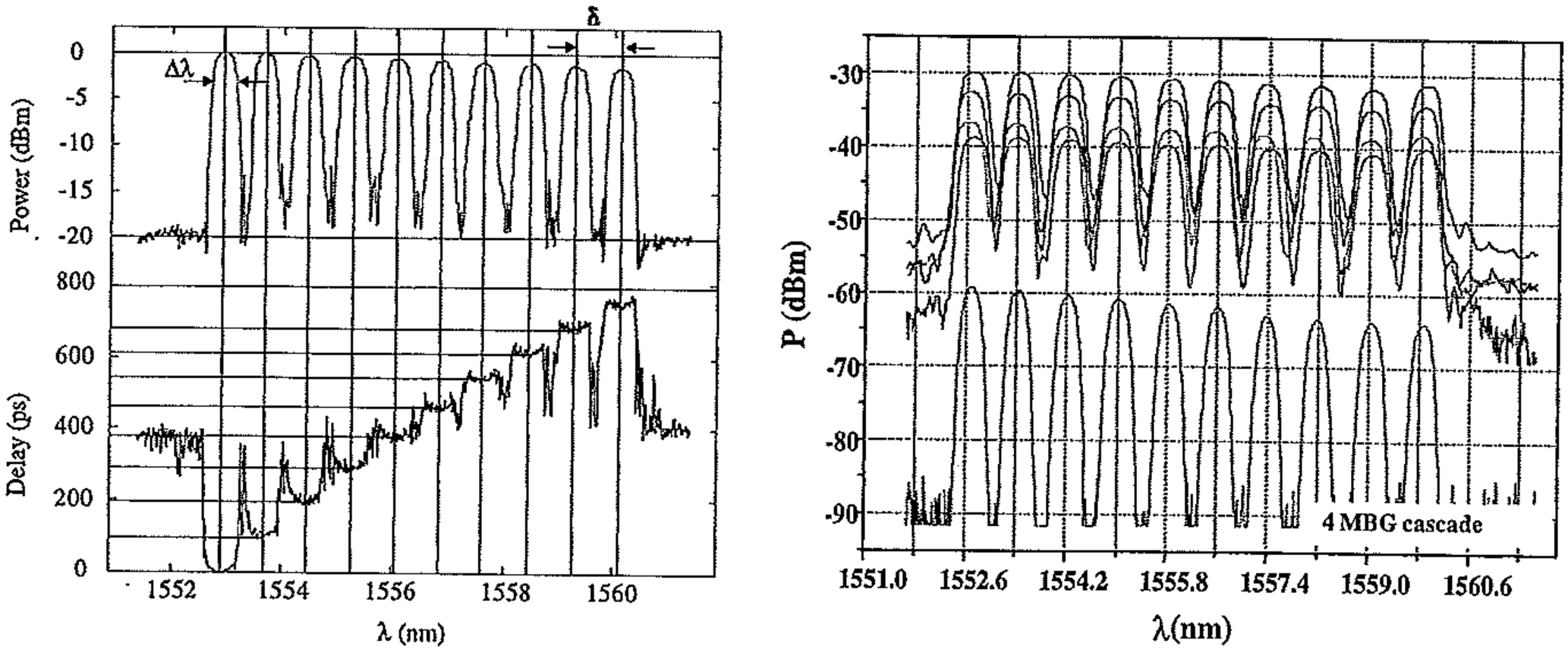

a) *b)*

Fig.6: BGA of consisting of 10 Bragg gratings spaced by 100 GHz a) reflected power spectrum and reflection delay from one Bragg grating set and b) reflected power spectra of four identical BGA and the resulting spectrum measured for the four BGA placed in cascade with circulators.

The reflected power spectra from the cascade of the four BGA was measured by combining the gratings with optical circulators and is shown in Fig.7b. The 3 dB FWHM of the cascade reflection peaks was 0.2±0.01 nm, a substantial reduction when compared to the single grating FWHM of 0.42 nm. The delays measured within the reflection bands are shown in Fig.7 for a single BGA and for the cascade of four BGA. It can be seen that the out of band dispersion, and possibly the noise on the grating profiles, introduced important perturbations on the channels last reflected from the arrays[20-21]. The variations in the delays predicted by numerical calculations are presented in Fig.8 using the sinc main lobe apodisation profile. Comparison with numerical simulations indicate that the larger oscillations observed in the experimental delay might result from the apodisation function being slightly truncated. The experimental delay curves were measured with 10 pm steps using a tuneable CW laser source modulated at 1 GHz and a network analyser. It is likely that the modulation frequency was too high to detect the high frequency oscillations in the delay curves displayed in the simulations for the last gratings. These BGA were inserted between the 5x100 km of a 10x10 Gb/s transmission system. The walk-off between the channels resulting from the time delays induced by the BGA successfully reduced the power penalty caused by XPM[3]. Detailed results of this experiment will be reported elsewhere.

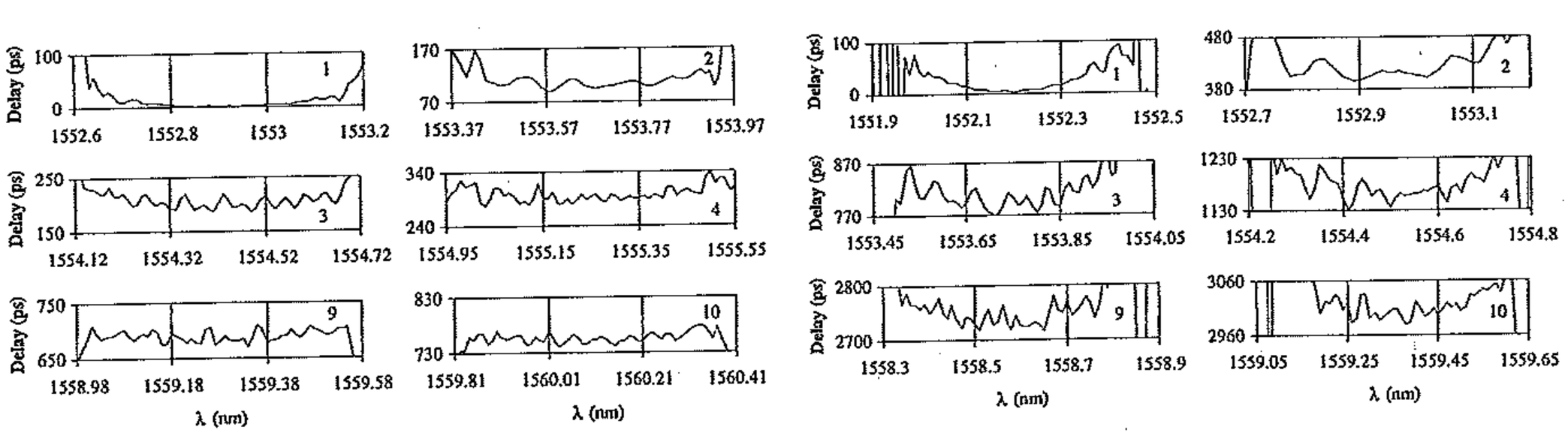

Fig.7: Delays as a function of the wavelength measured in the reflection band for six reflection peaks (corresponding to the Bragg gratings 1, 2, 3, 4, 9 and 10) for a) a single BGA and b) the four BGA cascade.

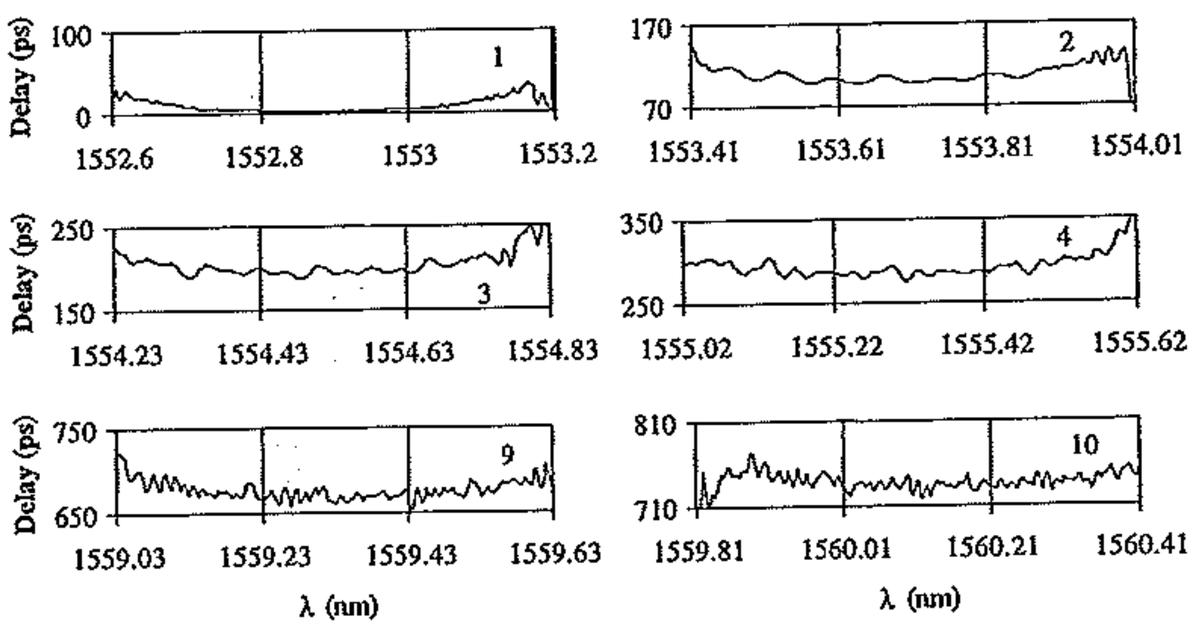

Fig.8: Reflection delays calculated for a BGA made of 10 Bragg gratings of 5 mm length with sinc apodisation, peak separation of 100 GHz and grating spacing varying from 10.1 mm to 6.6 mm.

4. Applications of BGA

In the previous section, it was mentioned that BGA efficiently suppressed XPM between co-propagating channels in 10 Gb/s WDM systems[3]. Gain equalisation within ± 0.1 dB was demonstrated using BGA, written with a different technique, inserted in the mid-section of a double-stage amplifier[22]. It therefore seems possible to realise BGA to simultaneously performed these two functions. Spectral analysis of optical pulses has also been demonstrated by introducing larger delays between the gratings. In their experiment, Hagemann et al. wrote 3600 gratings over 45 m of fibre as it is was drawn[23]. Spectral analysis

of ps pulses was thus performed by introducing more than 100 ns time delay between the frequency components of the 6 nm pulse bandwidth. Delays as small as 2 ps were also induced using superposed gratings for processing of microwave signals[24].

The time-frequency relation of BGA also allows the encoding of transmitted signal for OCDMA applications. OCDMA relies on the encoding of the transmitted signal to maximise the utilisation of the communication system resources, typically with packetised traffic. Sharing of the frequency space is achieved by assigning orthogonal, or nearly orthogonal, codes to each user. The design and optimisation of a family of codes is a complex task that will not be discussed here. It should however be mentioned that coding of the transmitted signal can be performed either in the time domain and/or the frequency domain. Time encoding, or direct sequence, OCDMA has been realised by the introduction of delay lines, using optical fibre lines or sampled Bragg gratings[25-28]. Reconfigurable codes were also obtained by strain-tuning the gratings[28]. Frequency encoding has been reported using optical Fourier transform and filtering of the optical spectrum with bulk optics[29] or fibre Mach-Zehneder interferometers with different free spectral range[30]. Fibre Bragg gratings encoders have also been realized with MoirØ gratings[31] and chirped gratings[32].

In 1997, it was proposed to achieve simultaneous encoding in both the frequency and time domains, or fast-frequency hopping, using series of Bragg gratings[33]. Later analysis of the system showed that the flexibility introduced by the two-dimensional coding space should result in an increase of the system capacity when compared to other systems relying on a one-dimensional coding space[4]. The all-fibre encoders also display lower losses than bulk optics encoders/decoders. The coding principle is presented in Fig.9. The bit sequence modulates a broadband CW source. The BGA encoder selectively reflects pre-determined wavelength bands and introduces delays between the reflected pulses at each wavelength. At the receiver, the decoder consists of a BGA identical to the encoder but placed in reverse order. The pulses from the desired encoder (i.e., that matching the decoder) are therefore resynchronised while the pulses from the interfering user (with non-matching encoders) are dispersed.

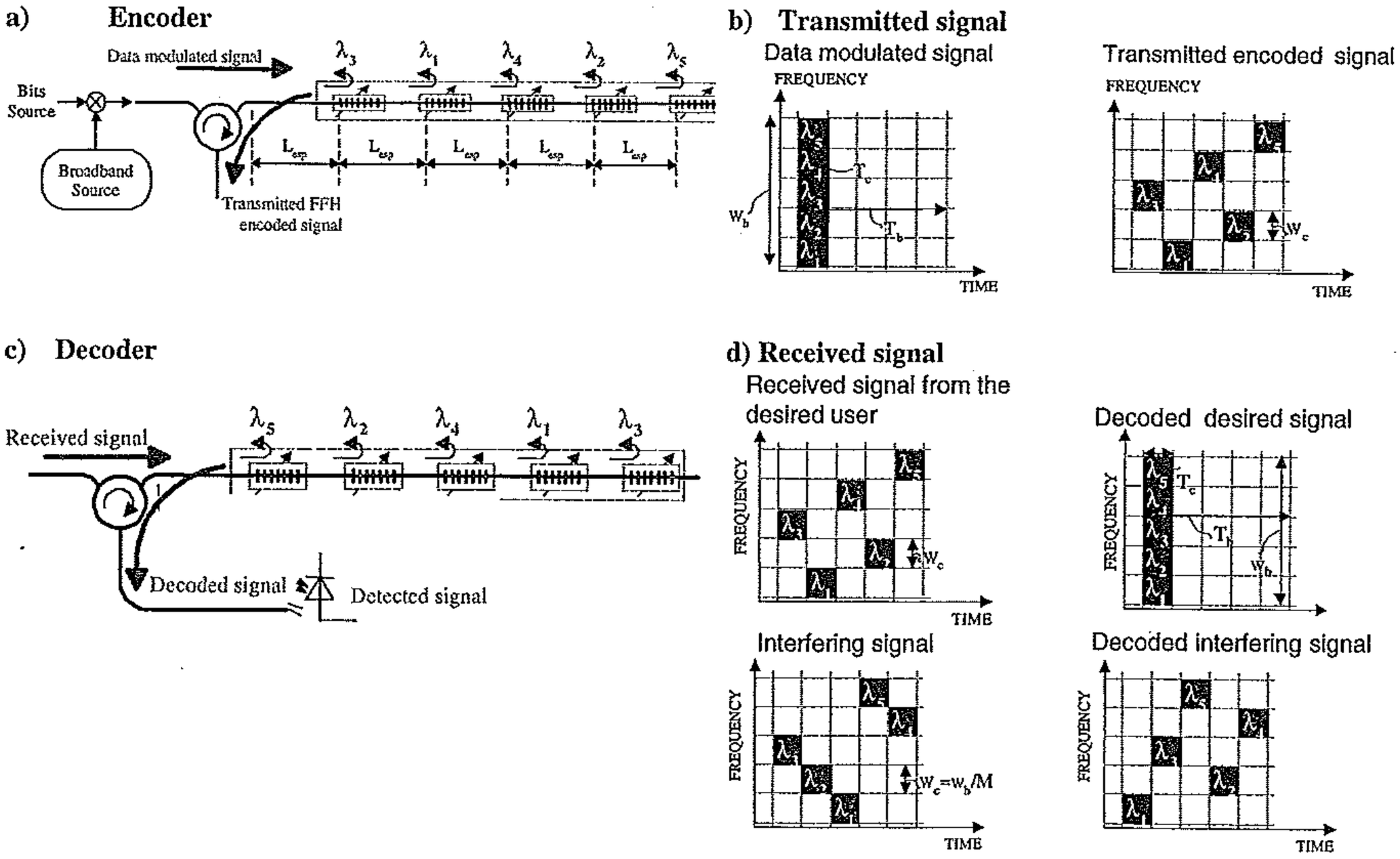

Fig. 9 Encoding and decoding of OCDMA using BGA showing a) the encoder, b) the transmitted signal, c) the decoder with Bragg wavelengths placed in reverse order to that of the encoder and c) the received signal showing the recombination of the desired user pulse and the dispersion of the interferer.

The design of the BGA strongly influences the performance of the system in terms of bit rate, capacity and transmission quality. The bit rate of the system is related to the length of the encoder since the data pulse has to exit the encoder before another pulse enters; high bit rate system therefore require short encoders. Encoder for 1 Gb/s system must be shorter than 10 cm. The number of gratings in the BGA is determined by the width of the data pulse related to the chip rate. Transmission of 100 ps pulses results in grating spacing of 10 mm. Therefore, at transmission rate of 1 Gb/s with 100ps pulses, a given code will have at most 10 wavelengths. However the capacity of the system, or the number of orthogonal codes, will depend on the total number of available wavelength bands. Narrow-band gratings will therefore result in a larger number of possible codes at the expense of a reduction of the transmitted power. Furthermore, the Bragg wavelengths and the longitudinal spacing of the encoder BGA and the decoder BGA must be perfectly matched to increase the signal to noise ratio.

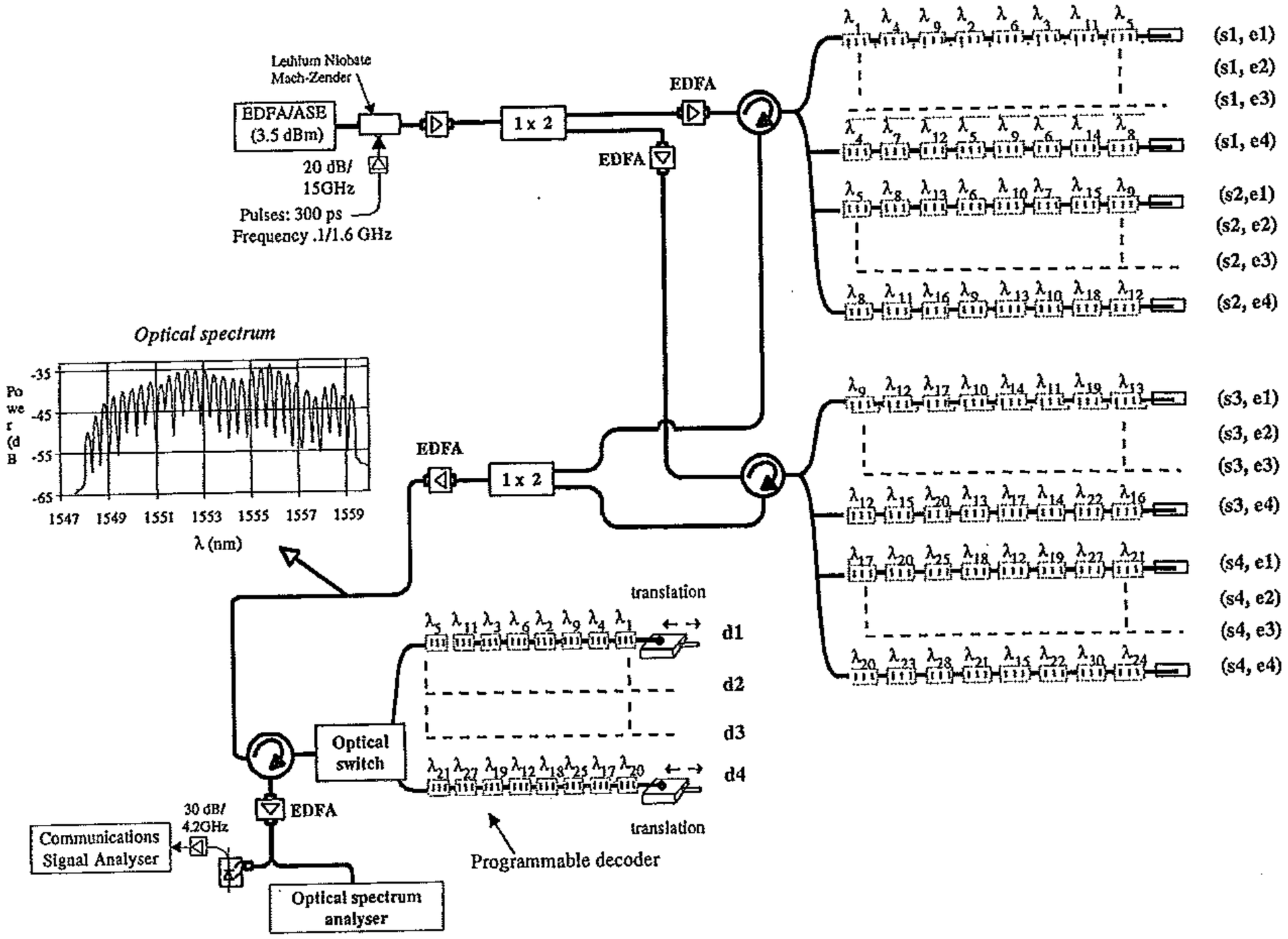

Fig. 9: OCDMA system with sixteen BGA encoders and four BGA decoders.

Sixteen encoders and four decoders consisting of BGA with eight gratings were written using the previously described Sagnac interferometer. The frequency spacing of the available wavelength bands was 50 GHz and the wavelength range extended from 1548.2 nm to 1559.6 nm. Each individual grating was 14 mm long with a sinc apodisation function. The grating were placed every 15 mm and the total encoder length was 12 cm. Ideally, the pulses reflected by each gratings should be separated in time, and therefore this system should be used with pulses shorter than 150 ps. Also, the total encoder length corresponds to a bit rate of length of 800 Mb/s. Thereflectivities and time delays of a BGA is displayed in Fig.10. The sixteen encoders were divided in four series (s1 to s4). Each of these series in fact consisted of four identical BGA that could be strain-tuned to change the code from e1 to e4, shifting the reflection spectrum by 0.4 nm between each code. Therefore, as displayed in Fig.9, only four programmable decoders were needed, one for each serie, to retrieve the signals. The first encoder of each series, with the associated codes, are presented in Fig.11. Further details on the selected codes, experimental setup and more comprehensive results will be presented elsewhere[34]. Received data at 800 Mb/s is displayed in Fig.12. The interference form the undesirable users is clearly seen. However, because of limitations of the available equipment, it should be noted that the data pulses had a 300 ps width rather than the required 150 ps for which the system was designed. It should

also be observed that, in FFH-CDMA systems, the thresholding takes place during the chip time thereby eliminating the interference occurring at other time slots.

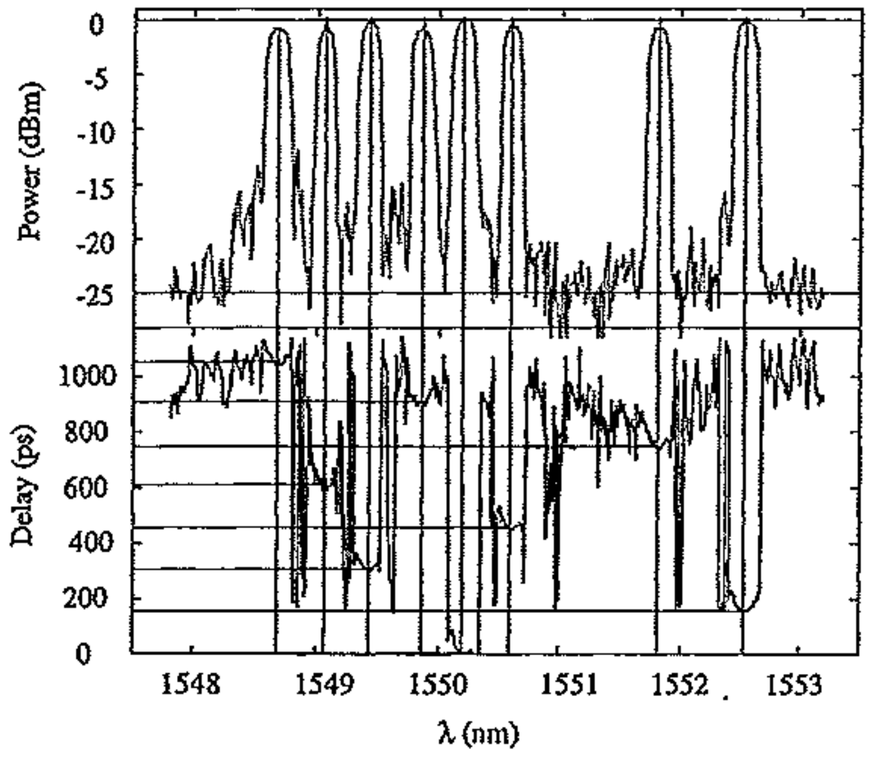

Fig. 10 Reflectivities and time delays of a BGA used in encoder serie s2.

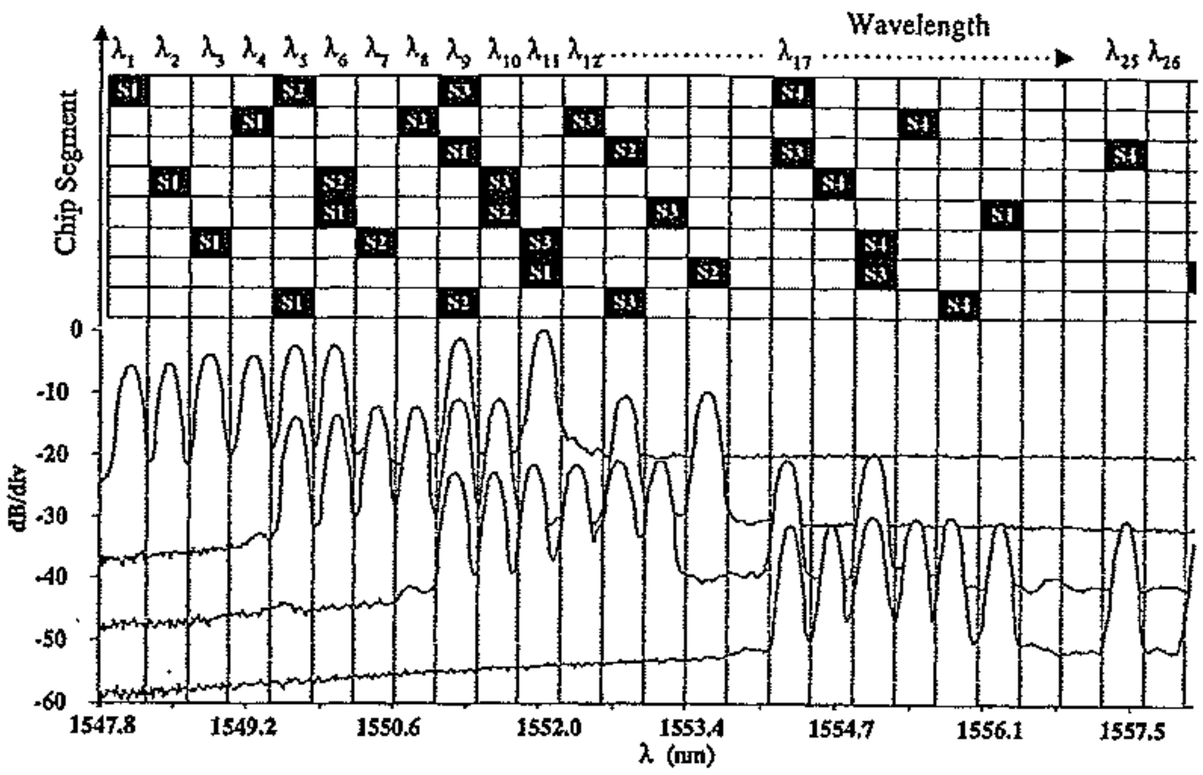

Fig. 11 Codes and spectra of the first encoder, e1, of each series (s1 to s4). Other encoders are obtained by strain tuning of similar gratings.

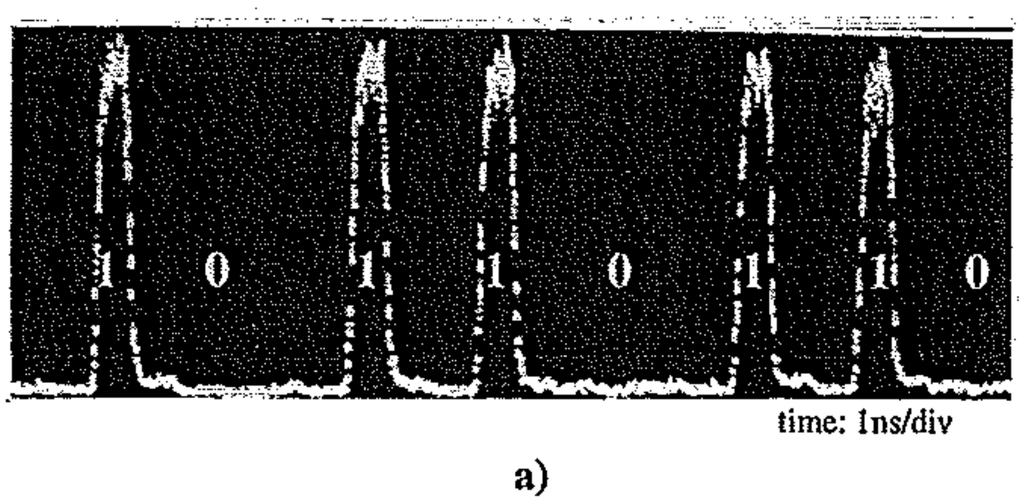

Fig. 12 Transmission at 800 Mb/s a) with only one user transmitting and b) with all users transmitting and the decoder tuned to (s4,e2).

5. Conclusion

Many applications relying on the time delays introduced between the reflected frequencies of successive narrow-band Bragg gratings have recently been proposed or demonstrated. Although these BGA can be written with a variety of techniques, the Sagnac-type interferometer offers great flexibility in the choice of Bragg wavelength, apodisation profile and grating length. This method offers an economical alternative to phasemask scanning techniques requiring multiple phasemasks. It is also simpler than other interferometric methods when cm-length gratings are required. Using BGA, temporal walk-off has been induced between co-propagating WDM channels to lower the penalties resulting from cross-phase modulation. In this case, the Bragg wavelengths are placed in increasing order with decreasing time delays between the channels. BGA also allow optical implementation of fast frequency hopping CDMA by providing the choice of frequencies and time delays to realise a two-dimensional code. Encoders and decoders have been achieved by positioning the gratings at constant spatial intervals along the fibre and by selecting the Bragg wavelength according to a pre-determined code. Data transmission at 800 Mb/s has been observed with sixteen simultaneously transmitting users using BGA encoders/decoders with eight reflected frequency bands.

6. Acknowledgements

This research was supported by the *Conseil de recherches en sciences naturelles et en gØnie* du Canada (CRSNG), *QuØbecTel*et le *Fonds pour la formation de chercheurs et laide la recherche* du QuØbec (FCAR).The authors are grateful to F. Ouellette for his inputs on the use of the Sagnac interferometer, P. Loiselle and . Tremblay for their help on the data acquisition software and J.-P Bouchard for his help with the simulation software.

7. References

1. K. O. Hill and G. Meltz, "Fiber Bragg grating technology fundamentals and overview", J. ofLightwave Technology. **15,** pp. 1263-1276, 1997.
2. C. R. Giles, "Lightwave applications of fiber Bragg gratings", J. ofLightwave Technology **15,** pp. 1391-1404, 1997.
3. G. Bellotti, S. Bigo, S. Gauchard, P.-Y. CortŁs and S. LaRochelle, "10x10 Gb/s cross-phase modulation suppressor using WDM narrowband fiber Bragg gratings", Optical fiber communication conference (OFC2000), paper PD32, 2000.
4. H. Fathallah, L.A. Rusch and S. LaRochelle, "Passive Optical-Hop CDMA Communications System", J. of Lightwave Technology **17**, pp. 397-405, 1999.
5. H. Fathallah, P.-Y. CortŁs, L.A. Rusch, S. LaRochelle and L. Pujol, "Experimental demonstrations of optical fast frequency hopping-CDMA communications", European Conference on Optical Communications (ECOC'99) **vol.I,** pp.190-191 (1999).
6. G. Meltz, W.W. Morey and W.H. Glenn, " Formation of Bragg gratings in optical fibers by a transverse holographic method", Optics Letters **14**, pp. 823-825 (1989).
7. R. Kashyap, J. R. Armitage, R. Wyatt, S.T. Davey and D. L. Williams, All-fibre narrow-band reflection gratings at 1500 nm, Electron.Lett. **26**, pp.730-731, 1990.
8. M. Farries, K. Sugden, D. Reid, I. Bennion, A. Molony and M.Goodwin, "Broad reflection bandwidth chirped fibre gratings and narrow bandpass filters produced by the use of an amplitude mask", Electron. Letters **30**, pp. 891-892 (1994).
9. P.-Y. Fonjallaz, B. Sahlgren, B. Grennbert and R. Stubbe, "New interferometer for complete design of UV-written fibre Bragg gratings", OSA Technical Digest Series (BGPP97)**17** , pp. 36-38, 1997.
10. K.O. Hill, B. Malo, F. Bilodeau, D.C. Johnson and J. Albert, "Bragg gratings fabricated in monomode photosensitive optical fiber by UV exposure through a phase mask", Appl. Phys. Lett. **62**, pp. 1035-1037 (1993).
11. J. Martin and F. Ouellette, "Novel writing technique of long and highly reflective infibre gratings", Electronics Letters **30**, pp. 811-812 (1994).
12. A. Othos and X. Lee, Novel and improved method of writing Bragg gratings with phase masks, IEEE Photonics Technology Letters **7**, pp.1183-1185 (1995).
13. Y. Painchaud, A. Chandonnet and J. Lauzon, "Chirped fibre gratings produced by tilting the fibre", Electronics Letters **31**, pp. 171-172 (1995).
14. K.C. Byron and H.N. Rourke, "Fabrication of chirped fibre gratings by novel stretch and write technique", Electronics Letters **31**, pp. 60-61 (1995).
15. J.D. Prohaska, E. Snitzer, S. Rishton and V. Boegli, "Magnification of mask fabricatedfibre Bragg gratings", Electron. Letters **29**, pp.1614-1615 (1998).
16. M.J. Cole, W.H. Loh, R.I. Laming, M.N. Zervas and S. Barcelos, "Moving fibre/phase mask-scanning beam technique for enhanced flexibility in producing fibre gratings with uniform phase mask", Electron. Letters **31**, pp. 1488-1490 (1995).
17. F. Ouellette and P. A. Krug, Writing ring interferometer for writing gratings, Australian patent AU7686896A1 (1997).
18. R. Kashyap, "Assessment of tuning the wavalength of chirped and unchirped fibre Bragg grating with single phase-masks", Electronics Letters **34**, pp. 2025-2027 (1998).
19. P.-Y. CortŁs, F. Ouellette and S. LaRochelle, "Intrinsic apodisation of Bragg gratings written using UV-pulse interferometry", Electronics Letters **34**, pp. 396-397 (1998).
20. J. E. Sipe, B. J. Eggleton and T. A. Strasser, Dispersion characteristics of nonuniform Bragg gratings: implications for WDM communication systems, Opt. Commun. **152**, pp. 269-274, 1998.
21. F. Ouellette, The effect of profile noise on the spectral response of fiber gratings, OSA Technical Digest Series (BGPP97) **17**, Washington DC, p. 222-224, 1997.
22. M. Rochette, M. Guy, S. LaRochelle, J. Lauzon and F. TrØpanier, "Gain equalization ofEDFA's with Bragg gratings", IEEE Photonics Technology Letters **11**, pp. 536-538 (1999).

23. V. Hagemann, M. Rothhardt and G. Sluyterman, "Step chirped draw tower grating arrays for spectral analysis of short pulses", ThE5-1, pp. 60-62 (1999).
24. G.W. Yoffe, K.E. Almeh and R.A. Minasian, "Superposed WDM fiber grating unit for short time-delay processing of signals", Microwave and Optical Technology Letters**24**, pp. 390-391 (2000).
25. J. Salehi, "Code division multiple access in techniques in optical fiber networks-Part I: Fundamental principles", IEEE Trans. Commun. **37**, p.824, 1998.
26. H. Geiger, A. Fu, P. Petropoulos, M. Ibsen, D.J. Richardson and R.I. Laming, "Demonstration of a Simple CDMA Transmitter and Receiver Using Sampled Fibre Gratings", European Conf. Opt. Com.(ECOC 1998), pp. 337-338 (1998).
27. G.E. Town, K. Chan and G. Yoffe, "Design and performance of high-speed optical pulse-code generators using optical fiber Bragg gratings", IEEE Journal of Selected Topics in Quantum Electronics**5**, pp. 1325-1331 (1999).
28. D.B. Hunter and R.A. Minasian, "Programmable high-speed optical code recognition using fibre Bragg grating arrays", Electronics Letters **35**, pp. 412-414 (1999).
29. D. Zaccarin and M. Kavehrad, An optical CDMA system based on spectral encoding of LED, IEEE Photon. Technol. Lett. **4**, pp. 479-482, 1993.
30. T. Pfeiffer, B. Deppisch and M. Witte, Transmission of Broadband coherence multiplexed signals over long distance fibre feeder, European Conference on Optical Communications (ECOC99) **vol I**, pp.186-187, 1999.
31. L.R. Chen, Smith PWE and CM de Sterke, "Wavelength-encoding/temporal-spreading optical code division multiple-access system with in-fiber chirped moire gratings", Applied Optics **38**, pp. 4500-4508 (1999).
32. A. Grunnet-Jepsen, A.E. Johnson, E.S. Maniloff, T.W. Mossberg, M.J. Munroe and J.N. Sweetser, "Fibre Bragg grating based spectral encoder/decoder for lightwave CDMA", Electronics Letters**35**, pp. 1096-1097 (1999).
33. H. Fathallah, S. LaRochelle and L. A. Rusch, Analysis of an optical frequency hop encoder using strain-tuned Bragg Gratings, OSA Technical Digest Series (BGPP97) **17**, Washington DC, p. 200-202, 1997.
34. H. Fathallah, P.-Y. CortŁs, H. Ben Jaafar, L.A. Rusch and S. LaRochelle, "Optical Fast Frequency Hopping- (OFFH-) CDMA: System Capacity and Experimental Advances", submitted to IEEE Journal of Lightwave Technology: Special Issue on optical Networks, 2000.